HOKKAIDO UNIVERSITY

Title	Visible Electroluminescence from n-Type Porous Silicon/Electrolyte Solution Interfaces : Time-Dependent Electroluminescence Spectra
Author(s)	Noguchi, Hidenori; Kondo, Toshihiro; Murakoshi, Kei et al.
Citation	Journal of The Electrochemical Society, 146(11), 4166-4171 https://doi.org/10.1149/1.1392608
Issue Date	1999
Doc URL	https://hdl.handle.net/2115/50238
Rights	© The Electrochemical Society, Inc. 1999. All rights reserved. Except as provided under U.S. copyright law, this work may not be reproduced, resold, distributed, or modified without the express permission of The Electrochemical Society (ECS). The archival version of this work was published in J. Electrochem. Soc. 1999 volume 146, issue 11, 4166-4171.
Type	journal article
File Information	JES146-11_4166-4171.pdf

Hokkaido University Collection of Scholarly and Academic Papers : HUSCAP



Journal of The Electrochemical Society

Visible Electroluminescence from n–Type Porous Silicon/Electrolyte Solution Interfaces: Time –Dependent Electroluminescence Spectra

Hidenori Noguchi, Toshihiro Kondo, Kei Murakoshi and Kohei Uosaki

J. Electrochem. Soc. 1999, Volume 146, Issue 11, Pages 4166-4171.
doi: 10.1149/1.1392608

Email alerting service Receive free email alerts when new articles cite this article - sign up in the box at the top right corner of the article or click here

To subscribe to *Journal of The Electrochemical Society* go to:
http://jes.ecsdl.org/subscriptions

© 1999 ECS - The Electrochemical Society

Downloaded on 2012-09-26 to IP **133.87.26.18** address. Redistribution subject to ECS license or copyright; see **www.esltbd.org**

Journal of The Electrochemical Society, **146** (11) 4166-4171 (1999)
S0013-4651(99)04-064-1 CCC: $7.00 © The Electrochemical Society, Inc.

Visible Electroluminescence from n-Type Porous Silicon/Electrolyte Solution Interfaces: Time-Dependent Electroluminescence Spectra

Hidenori Noguchi, Toshihiro Kondo, Kei Murakoshi, and Kohei Uosaki*,z

Physical Chemistry Laboratory, Division of Chemistry, Graduate School of Science, Hokkaido University, Sapporo 060-0810, Japan

Visible electroluminescence (EL) from n-type porous silicon (n-PS) in an electrolyte solution containing $S_2O_8^{2-}$ was investigated by potential-sweep and potential-step methods. Potential sweep measurements showed that both the cathodic current and EL intensity increased and the EL spectra blue-shifted as the potential became negative. These characteristics were further studied by the potential-step method. Immediately after the potential was stepped to a negative value, the cathodic current began to flow and EL was observed. The EL intensity then increased but the cathodic current decreased with time. The rate of the increase in the EL intensity depended not on the $S_2O_8^{2-}$ concentrations but on the applied negative potentials. Time-resolved EL spectra measurements showed that the EL spectrum was blue-shifted with time even when a constant negative potential was applied to n-PS. These results were explained by considering that the emission site was changed from larger-sized Si crystallites to smaller-sized ones in the n-PS layer with time.
© 1999 The Electrochemical Society. S0013-4651(99)04-064-1. All rights reserved.

Manuscript submitted April 19, 1999; revised manuscript received June 20, 1999.

Since Canham[1] reported visible photoluminescence (PL) from porous silicon (PS), many studies on PS have been carried out from various aspects because of the possible development of Si-based optoelectronic devices.[2-7] The origin of the visible light emission is considered due to the quantum size effect,[8-10] although several alternative models have been proposed.[11-14]

Most of the studies reported so far have concentrated on the PL properties of PS.[15-22] Electroluminescence (EL) is, however, more important as far as technological application is concerned. In this respect, Koshida and Koyama demonstrated that a transparent metal/PS/p-Si/Al cell emits EL (orange) at relatively low applied voltage, although the quantum efficiency was quite low ($<10^{-5}$%).[2]

The study of EL properties of semiconductor/electrolyte solution interfaces has been known to be very valuable in the characterization of the interfaces.[23-28] This must also be the case for PS/electrolyte solution interfaces. Visible EL from a PS/electrolyte solution interface can be obtained under both anodic and cathodic polarization, depending on the doping type of the substrate. For p-type porous silicon (p-PS), light emission is observed during anodic oxidation in aqueous electrolyte solution.[29-35] In previous papers we investigated the relation between the chemical nature and EL properties of p-PS by *ex situ* X-ray photoelectron spectroscopy (XPS)[36] and *in situ* Fourier transform infrared spectroscopy (FTIR)[33,34] measurements and proved quantitatively that surface Si-H_n species contribute to EL. In the case of n-PS, EL is obtained when the n-PS is cathodically biased in an electrolyte containing an electroactive species which can inject holes into the valence band of the semiconductor.[37-48] It is known that if a negative potential is applied to an n-type semiconductor in a solution containing a hole injector such as $S_2O_8^{2-}$, EL is observed as a result of the following reactions[49]

$$S_2O_8^{2-} + e_c^- \rightarrow SO_4^{\cdot -} + SO_4^{2-} \quad [1]$$

$$SO_4^{\cdot -} \rightarrow SO_4^{2-} + p_v^+ \quad [2]$$

$$p_v^+ + e_c^- \rightarrow h\nu(\mathrm{EL}) \quad [3]$$

where e_c^- is an electron in the conduction band of an n-type semiconductor and p_v^+ is a hole injected from $SO_4^{\cdot -}$ to the valence band. This mechanism is expected to explain the visible EL from cathodically biased n-PS in contact with $S_2O_8^{2-}$ solution. Recently, Kooij *et al.*[47] investigated the electrochemical characteristics of PS in acidic $S_2O_8^{2-}$ solution in detail. Compared with results obtained on p-GaAs with p-PS, they observed no enhancement of the photocurrent, *i.e.*, photocurrent doubling due to the contribution of hole injection from $SO_4^{\cdot -}$ at p-PS in the presence of $S_2O_8^{2-}$ under reverse bias conditions. Because a similar effect might be occurring with an n-type electrode in $S_2O_8^{2-}$ solution, they suggested that the reduction of $S_2O_8^{2-}$ at PS electrodes is not always accompanied by hole injection into the valence band. However, the mechanism of the reduction of $S_2O_8^{2-}$ is still unclear. Thus, quantitative analysis of the application of this EL system to an n-PS/electrolyte solution interface must still be important. One of the most interesting characteristics in this system is the shift of the EL spectra to higher energy as the potential is scanned or stepped to negative values.[37-48] We have found, however, that the spectra of the visible EL from n-PS in an electrolyte solution containing $S_2O_8^{2-}$ blue-shifted with time even when a constant negative potential was applied to n-PS, contrary to the results previously reported.[46]

The present work was carried out to clarify the mechanism of the voltage-tunable blue shift of the EL from an n-PS/electrolyte solution interface by employing both potential-sweep and potential-step methods. The dependence of the intensity and spectra of the EL on electrode potential and $S_2O_8^{2-}$ concentrations as well as on time were investigated.

Experimental

Preparation of PS.—Silicon wafers used in these experiments were n-type (1.4-2.0 Ω cm) single crystals obtained from Shin-Etsu Semiconductor with a (100) surface. The wafers were cleaned first with acetone to remove organic impurities, washed with pure water, and then chemically etched in 10% HF-ethanol solution for 1 min. After ohmic contact was obtained using an In-Zn alloy, the samples were placed in an electrode holder made from Teflon so that only one face of the wafer was exposed (apparent exposed area, 0.283 cm^2). Constant current anodic oxidation was carried out in 10% HF-ethanol solution under illumination with a 30 W halogen lamp in order to provide holes which are required for the formation of a porous structure of n-PS. A potentiostat/galvanostat (Hokuto Denko, HA-151) was used to control the current, and a Pt wire was employed as a counter electrode. Current density for the porous formation was 5 mA/cm^2, and the oxidation time was varied from 10 to 1800 s. The as-prepared n-PS was rinsed with purified water and transferred to the spectroelectrochemical cell without exposure to air before the electrochemical and the EL measurements to prevent dryness[50] as well as native oxide growth.[51]

Electrochemical and EL measurements.—As-prepared n-PS samples were used for EL measurements only once, because one EL measurement alters the nature of the PS layer in certain cases. EL

* Electrochemical Society Active Member.
z E-mail: uosaki@PCL.sci.hokudai.ac.jp

Downloaded on 2012-09-26 to IP 133.87.26.18 address. Redistribution subject to ECS license or copyright; see www.esltbd.org

S0013-4651(99)04-064-1 CCC: $7.00 © The Electrochemical Society, Inc.

measurements were carried out in 0.2 M Na_2SO_4 solution containing 0-0.15 M $K_2S_2O_8$ in a three-electrode glass cell having an optical window. Ag/AgCl (sat. KCl) and a Pt wire were employed as the reference and counter electrodes, respectively. Electrolyte solution was prepared using reagent-grade Na_2SO_4 (Wako Pure Chemicals), $K_2S_2O_8$ (Wako Pure Chemicals), and Milli-Q water and was deaerated by passing high-purity nitrogen gas (99.99%) through it prior to the measurements. The potential was controlled using a potentiostat/galvanostat (Toho Technical Research, 2001) and a function generator (Hokuto Denko, HB-111). An external potential pulse was provided by a personal computer (NEC Corp., PC-8801 MH) through a 12-bit DA converter. Potential pulse width was 0.2-1 s. EL intensity was measured using a photomultiplier tube (PMT, Hamamatsu Photonics Co., Ltd., R1767). The applied voltage to the PMT was −0.75 kV, and the output signal was amplified using a homemade fast amplifier. The current and the amplified PMT signal were recorded using the personal computer through a 12-bit AD converter. EL spectra were obtained using a multichannel detector (Hamamatsu Photonics Co., Ltd., IMD-C3300) with an image intensifier combined with an imaging spectrograph (Jobin Yvon, CP-200; f = 2.9). The plasma-coupled-device (PCD) elements were cooled to −20°C. The exposure time was set from 0.1 to 0.2 s. The optical system is sensitive from 1.4 to 3.4 eV with a resolution of 4 nm. All the measurements were carried out in the dark at room temperature.

Results and Discussion

Current and EL characteristics obtained by the potential-sweep method.—Figure 1 shows the current-potential and the EL intensity-potential relations of an n-PS electrode which was prepared by anodic oxidation for 300 s in 0.2 M Na_2SO_4 solution containing 0.15 M $K_2S_2O_8$ measured by sweeping the potential in the negative direction at various scan rates. A cathodic current was observed at potentials more negative than −0.55 V. Limiting current was observed when the scan rate was 20 or 100 mV/s, but the current increased monotonously within the potential region employed in this study when the potential was scanned at 1000 mV/s. EL was observed at potentials more negative than −1.0 V in all cases. The EL intensities increased as the potential became negative when the scan rates were 20 and 100 mV/s, reached a maximum at −1.6 and −1.7 V, respectively, and then decreased rapidly after the EL peaks, although the cathodic current still flowed. No EL peak was observed within the potential region examined at 1000 mV/s scan. Although the behavior of both the EL intensity and cathodic current during the potential scan has been reported already by several groups,[37-48] they employed only one scan rate. It is clear from Fig. 1 that when the potential was scanned faster, the limiting values of the cathodic current and the EL intensity became higher for the reduction current and the EL. It was also found that the faster the potential was scanned, the more negative was the peak potential.

Figure 2 shows typical EL spectra observed at various negative potentials during a potential scan at 20 mV/s (cf. Fig. 1). Because the exposure time of the PCD was 5 s, each spectrum was obtained during the potential scan from −1.0 to −2.0 V at 0.1 V intervals. The peak energy of the EL spectra was blue-shifted from *ca*. 1.7 eV at −1.3 V to *ca*. 2.1 eV at −1.8 V. After the potential reached −1.8 V, however, the EL spectra were red-shifted (Fig. 2e and f). No potential dependence was observed for the low-energy threshold of the EL spectra. The voltage-tunable EL from the n-PS/electrolyte solution interface has already been reported by several groups[37-43] during a potential scan from −1.0 to −1.6 V. Very recently, Lim *et al*.[48] have reported that the peak of the EL spectra showed a red shift at a constant negative potential by repeating the potential application. They attributed this phenomenon to the bandgap lowering caused by the conversion of the predominant Si–H surface bonds to Si–Si bonds formed by the destruction of the surface bonds of PS. The red shift of the EL spectra during the negative scan observed in our experiments may be related to this effect.

Figure 3 shows the EL spectra observed at −1.5 V at various scan rates. The exposure time of PCD for 20, 100, and 1000 mV/s scans

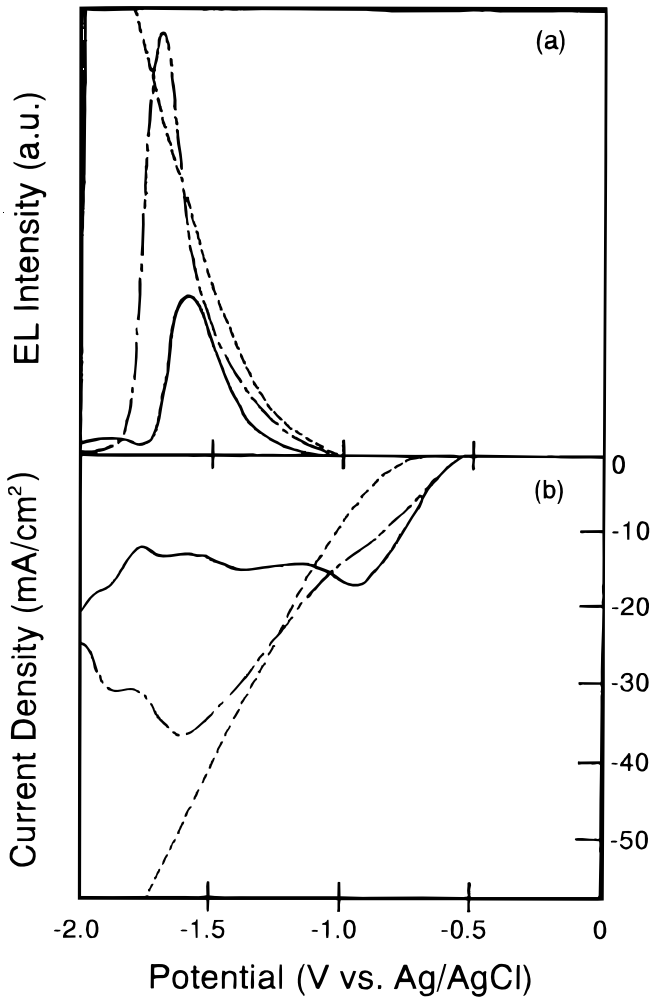


Figure 1. (a) EL intensity-potential and (b) current density-potential curves obtained in 0.2 M Na_2SO_4 and 0.15 M $K_2S_2O_8$ solution. n-PS samples were prepared by anodic oxidation in 10% HF-ethanol at 5 mA/cm^2 for 300 s. Potential scan rate was (—) 20 mV/s, (– – –) 100 mV/s, and (- - -) 1000 mV/s.

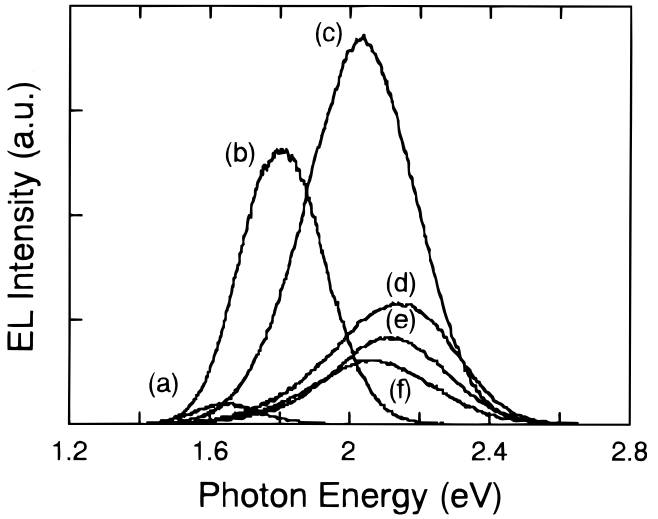


Figure 2. EL spectra obtained in 0.2 M Na_2SO_4 and 0.15 M $K_2S_2O_8$ solution during the potential scan from 0 to −2.0 V at (a) −1.0, (b) −1.2, (c) −1.4, (d) −1.7, (e) −1.8, and (f) −1.9 V. EL spectra were obtained in 0.1 s, potential scan rate was 20 mV/s. n-PS samples were prepared by anodic oxidation in 10% HF-ethanol at 5 mA/cm^2 for 300 s.

Downloaded on 2012-09-26 to IP 133.87.26.18 address. Redistribution subject to ECS license or copyright; see www.esltbd.org

S0013-4651(99)04-064-1 CCC: $7.00 © The Electrochemical Society, Inc.

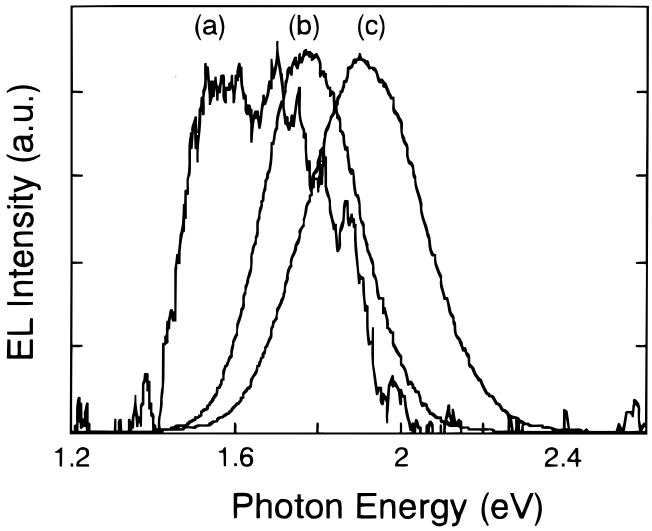


Figure 3. EL spectra obtained in 0.2 M Na_2SO_4 and 0.15 M $K_2S_2O_8$ solution at −1.5 V during the potential scan from 0 to −2.0 V at a potential scan rate of (a) 1000, (b) 100, and (c) 20 mV/s. EL spectra were obtained in 0.1 s.

were 5, 1, and 0.1 s, respectively, so that all spectra were observed at 0.1 V intervals. The peak intensity of the EL spectra was normalized to that of the data obtained at 20 mV/s. It is clear that the peak energy of the EL spectrum did not coincide in all cases, even when the same negative potential was applied to n-PS.

Figure 4 shows the relation between the peak energy and the applied negative potential. When the potential was scanned at 20 mV/s, the peak energy of the EL spectra increased in proportion to the applied negative potential with a slope of *ca*. 1 eV/V over a voltage range from −1.2 to −1.7 V, which is close to the value reported in the literature. If the scan rate was increased to 1000 mV/s, however, the peak energy of the EL spectra was almost constant during the negative potential scan.

Previously, Bsiesy *et al*.[40,41] have reported that the peak energy of the EL spectra is proportional to the applied negative potential with a slope of 1 eV/V when the potential was scanned at 25 mV/s. They proposed a model considering a quantum size effect in which an increase in ΔV is followed by an increase in the energy of emitted photons $\Delta h\nu = e\Delta V$ to explain the blue shift of the EL spectra. Very recently, however, Lim *et al*.[48] reported that this relation

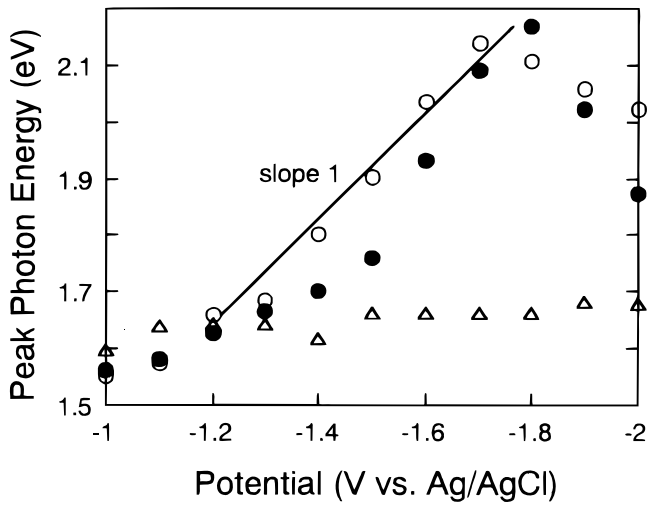


Figure 4. The dependence of peak energy on applied potential obtained during the potential scan from 0 to −2.0 V. Potential scan rate (○) 20, (●) 100, and (△) 1000 mV/s.

between the peak energy and the applied negative potential was very sensitive to the experimental conditions, *i.e.*, the slope changes with the different degrees of PS surface oxidation by $SO_4^{\cdot-}$. Hence, in the present study, as-prepared n-PS samples were used for EL measurements only once, because one EL measurement alters the nature of the PS layer in certain cases. It is clear from Fig. 4 that the peak photon energy was not related linearly to the applied potential and that the blue shift of the peak energy became smaller when the potential scan rate was higher than 20 mV/s, *i.e.*, when the duration of the potential application to n-PS became short, the blue shift of the EL spectra became definitely retarded. The present results suggest that the effect due to the time just after potential was applied to n-PS also plays an important role in the mechanism of the blue shift of the EL spectra.

Current and EL characteristics obtained by the potential-step method.—In order to understand the time dependence of the EL spectra in more detail, we carried out potential step measurements. Figure 5 shows the time profiles of the EL intensity and cathodic current of n-PS, which was prepared by anodic oxidation for 300 s, when the potential was stepped from 0 to a certain negative value in 0.2 M Na_2SO_4 containing 0.15 M $K_2S_2O_8$. When the pulse limit was −1.5 V or −2.0 V, EL began to be observed just after the potential step, and its intensity increased gradually to the end of the applied negative pulse. When the potential was stepped to −2.5 or −3.0 V, however, EL started to occur just after the potential step; its intensity increased dramatically with time, reached a maximum, and then decreased rapidly. Actually, similar trends were observed even when the potential was stepped to −1.5 and −2.0 V if the measurements were carried out over a longer time scale (Fig. 6a and b). The more negative the potential was stepped to, the faster the EL maximum appeared. When a negative potential was applied, cathodic current

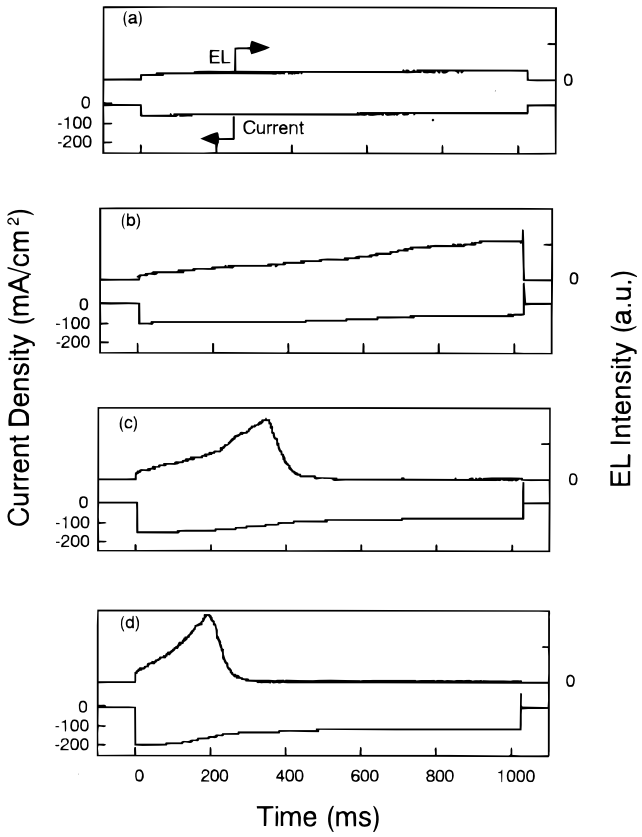


Figure 5. Time profiles of EL intensity and current density observed in 0.2 M Na_2SO_4 and 0.15 M $K_2S_2O_8$ solution. n-PS samples were prepared by anodic oxidation in 10% HF-ethanol at 5 mA/cm^2 for 300 s. Potential was stepped from 0 V to (a) −1.5, (b) −2.0, (c) −2.5, and (d) −3.0 V.

Downloaded on 2012-09-26 to IP 133.87.26.18 address. Redistribution subject to ECS license or copyright; see www.esltbd.org

S0013-4651(99)04-064-1 CCC: $7.00 © The Electrochemical Society, Inc.

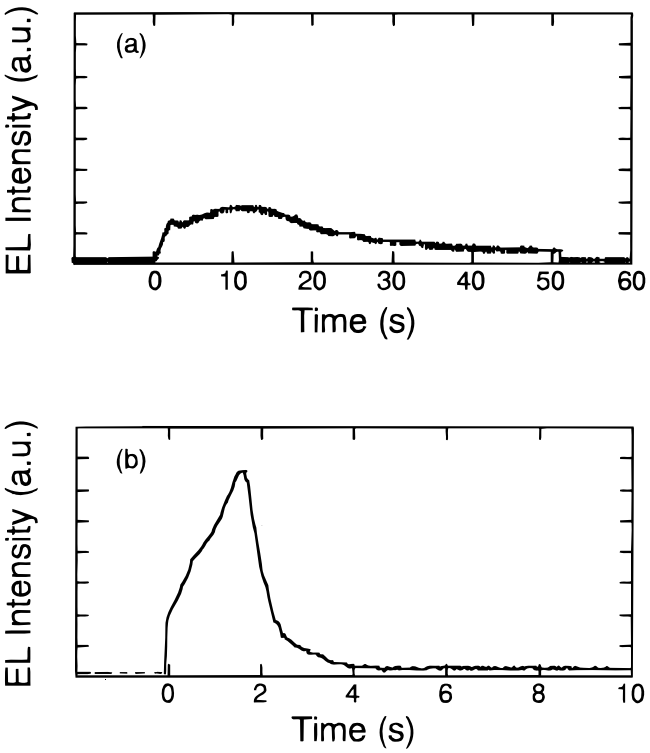


Figure 6. Time profiles of EL intensity on a larger time scale to (a) −1.5 and (b) −2.0 V in Fig. 5a and b.

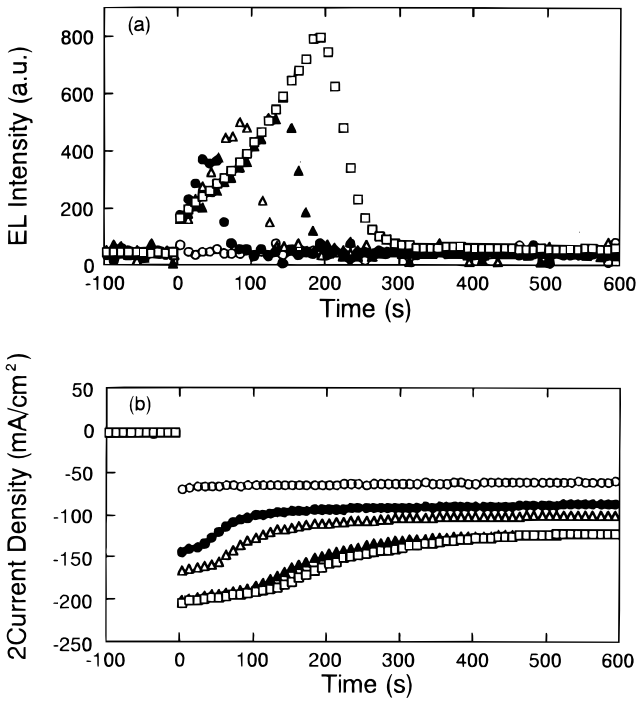


Figure 7. Time profiles of (a) EL intensity and (b) current density observed by potential stepping for 1 s from 0 to −3.0 V. Electrolyte solutions measured were 0.2 M Na_2SO_4 + (○) 0, (●) 0.05, (△) 0.075, (▲) 0.125, and (□) 0.15 M $K_2S_2O_8$ solutions. n-PS samples were prepared by anodic oxidation in 10% HF-ethanol at 5 mA/cm^2 for 300 s.

started to flow, decreased gently, showed an inflection point, and then decreased gradually. The time when the inflection point in the current time profile appeared was in good agreement with the time when the EL intensity reached a maximum.

Figure 7 shows the time profiles of EL intensity and cathodic current in 0.2 M Na_2SO_4 solution containing various concentrations of $S_2O_8^{2-}$. For all the cases in Fig. 7, the samples were prepared by anodic oxidation for 300 s and the potential was stepped from 0 to −3.0 V for 1 s. When $S_2O_8^{2-}$ was not present in the solution, EL from n-PS was not observed and the cathodic current reached a steady value almost immediately after the potential step, as shown in Fig. 7a. When $S_2O_8^{2-}$ was present in the electrolyte solution, EL started to occur just after a negative potential was applied. Its intensity increased gradually with time, reached a maximum, and decreased rapidly. The time when the EL intensity reached a maximum was in good agreement with the time the inflection point appeared in the current time profile. Concentrations of $S_2O_8^{2-}$ in the electrolyte solution influenced the rate of the increase in the EL intensity only slightly but significantly influenced the time to reach a maximum in the EL intensity time. The time to reach a maximum in the EL intensity profile was delayed, and therefore, the maximum EL intensity was higher as the $SO_4^{\cdot-}$ concentration became higher. As soon as the potential was stepped to a negative value, cathodic current started to flow, decreased gently, showed an inflection point, and decreased gradually as already reported in Fig. 5.

We considered the overall mechanisms of the electrochemical reaction occurring at the n-PS electrode during the potential step as follows:[52] (*i*) mass transport (*i.e.*, $S_2O_8^{2-}$ transport) to the n-PS electrode, (*ii*) electron transfer at the n-PS electrode surface (reaction 1 and 2), (*iii*) visible light emission (reaction 3).

In general, mass transport can be achieved by migration, convection, or diffusion. In the presence of a strong electrolyte and using a stationary electrode, both of which were used in our experiments, mass transport occurs only by diffusion. If the current observed in our potential-step measurements is diffusion-controlled, the depletion of $S_2O_8^{2-}$ near the n-PS electrode surface must be characterized by an inverse $t^{1/2}$ function, *i.e.*, current is in proportion to inverse $t^{1/2}$. [52] A Cottrell plot of the current and the EL intensity from the data in Fig. 5c and d is shown in Fig. 8. During the first stage of the potential step (region a), however, the current was almost constant although the EL intensity increased gradually. After the maximum of the EL intensity appeared (region b), both current and EL intensity were decaying linearly with inverse $t^{1/2}$. Thus, it is clear that EL proceeds by two different mechanisms before (region a), and after (region b) the EL intensity reached a maximum.

Let us discuss the EL mechanism before a maximum in the EL time profile (region a). In this region, EL intensity increased gradually with time just after a negative potential pulse was applied to the n-PS. In addition, this increase in the EL intensity was almost independent of the $S_2O_8^{2-}$ concentration (Fig. 7a). Hence, it is possible to say that in region (a), generation of EL is not limited by the diffusion of $S_2O_8^{2-}$ in the electrolyte. The Cottrell plot (Fig. 8) which did not show a linear dependence of current and inverse $t^{1/2}$ in region a may support this speculation. In region (a), thus, the generation of EL is limited by the electron flux supplied from the n-PS electrode. Recently, Gelloz *et al.*[53] reported that the PS layer in contact with an electrolyte is not always conductive but is also depleted of free carriers under some conditions. Thus, when negative potential pulse is applied to n-PS, an electric field emerges gradually from the n-PS/Si interface to the n-PS/electrolyte solution interface due to the high interfacial capacitace.[54] Finally, a homogeneous electric field through the n-PS layer forms and $S_2O_8^{2-}$ existing in the PS layer from the beginning of the potential pulse is reduced by the current until it becomes nearly zero. Thus, the EL intensity increases gradually with time in region (a). By making the potential more negative, the high driving force to build up a homogeneous electric field through the PS layer leads to both the time and the rate to reach a maximum in the EL time profile faster.

In the case of region b, a rapid decrease in the EL intensity after the maximum was observed. In this region, current and inverse $t^{1/2}$ showed a linear relationship, which means that when the electrochemical reaction is diffusion-controlled, $S_2O_8^{2-}$ is depleted at the surface and eventually $SO_4^{\cdot-}$ also decreases. That is the reason the EL intensity decreases in region b.

Downloaded on 2012-09-26 to IP 133.87.26.18 address. Redistribution subject to ECS license or copyright; see www.esltbd.org

S0013-4651(99)04-064-1 CCC: $7.00 © The Electrochemical Society, Inc.

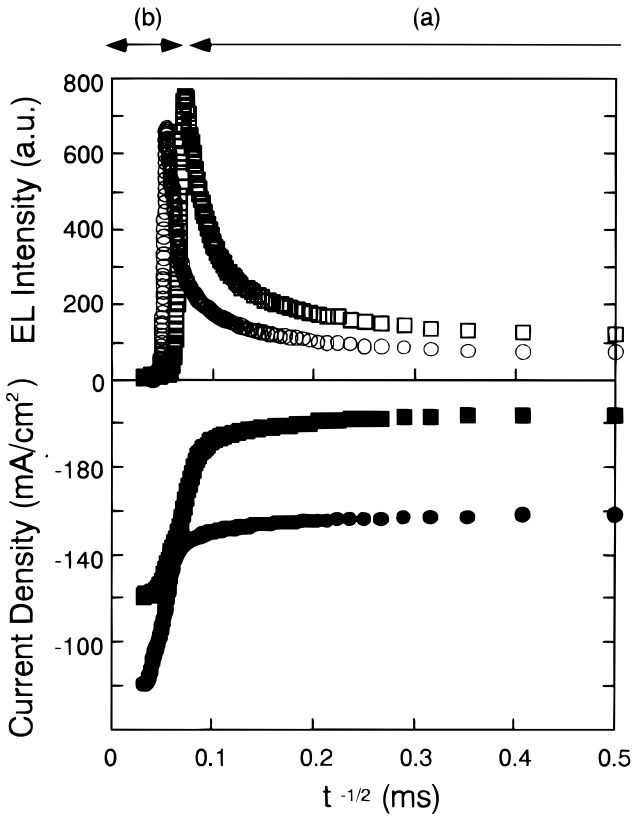


Figure 8. A Cottrell plot of the current [(●) −2.5 and (■) −3.0 V] and the EL intensity [(○) −2.5 and (□) −3.0 V] from the data in Fig. 5d, c. See text for details.

Time-dependent EL spectra.—Figure 9 shows the typical time-resolved EL spectra from n-PS, which was prepared by anodic oxidation for 300 s, obtained every 0.1 s after the potential was pulsed to −2.0 V in 0.2 M Na_2SO_4 containing 0.15 M $K_2S_2O_8$.[46] The peak energy and the high energy threshold of the EL spectrum showed a blue shift during a constant negative potential application, although the low-energy threshold was constant (*ca*. 1.4 eV).

Figure 10 shows the relationship between the peak energy and time after stepping the potential from 0 V to a certain negative value. The data in Fig. 10 were obtained in 0.2 M Na_2SO_4 containing 0.15 M $K_2S_2O_8$ using an n-PS sample prepared by anodic oxidation for 300 s. The peak energy was blue-shifted from *ca*. 1.5 eV observed just after cathodic polarization to higher values as time proceeded. It is interesting to note that the maximum peak energy was *ca*. 2.1 eV in all cases, except for the case when the potential was pulsed to −1.5 V where a negligible peak shift was observed. Clearly, the more negative the applied potential, the faster is the rate of the blue shift of the peak energy. The high-energy threshold showed similar trends. We emphasize here that the EL spectra from n-PS showed a blue shift with time even when a constant negative potential was applied and the maximum peak energy was almost independent of the applied potential. Note that the time region of these blue shifts coincides with that of the increase in EL intensity as shown in Fig. 5.

Mechanism for blue shift of EL with time.—The blue shift of the EL spectra has been reported by several groups under conditions similar to ours. Their explanations for the blue shift were mainly based on considering the size distribution of the nanometer-sized Si crystallites, which produce the quantum size effect.

If a visible EL from n-PS is due to the quantum size effect of the spatial confinement of the charge carriers in the nanometer-sized Si crystallites, the EL spectrum obtained from n-PS reflects the size distribution of the nanometer-sized Si crystallites in the n-PS layer and the peak energy of the EL spectrum provides the bandgap energy of the Si crystallites with the most dominant nanometer-size in n-PS. The fact that the peak energy and the high-energy threshold blue-shifted from *ca*. 1.5 to *ca*. 2.0 eV and from *ca*. 1.6 to *ca*. 2.6 eV,

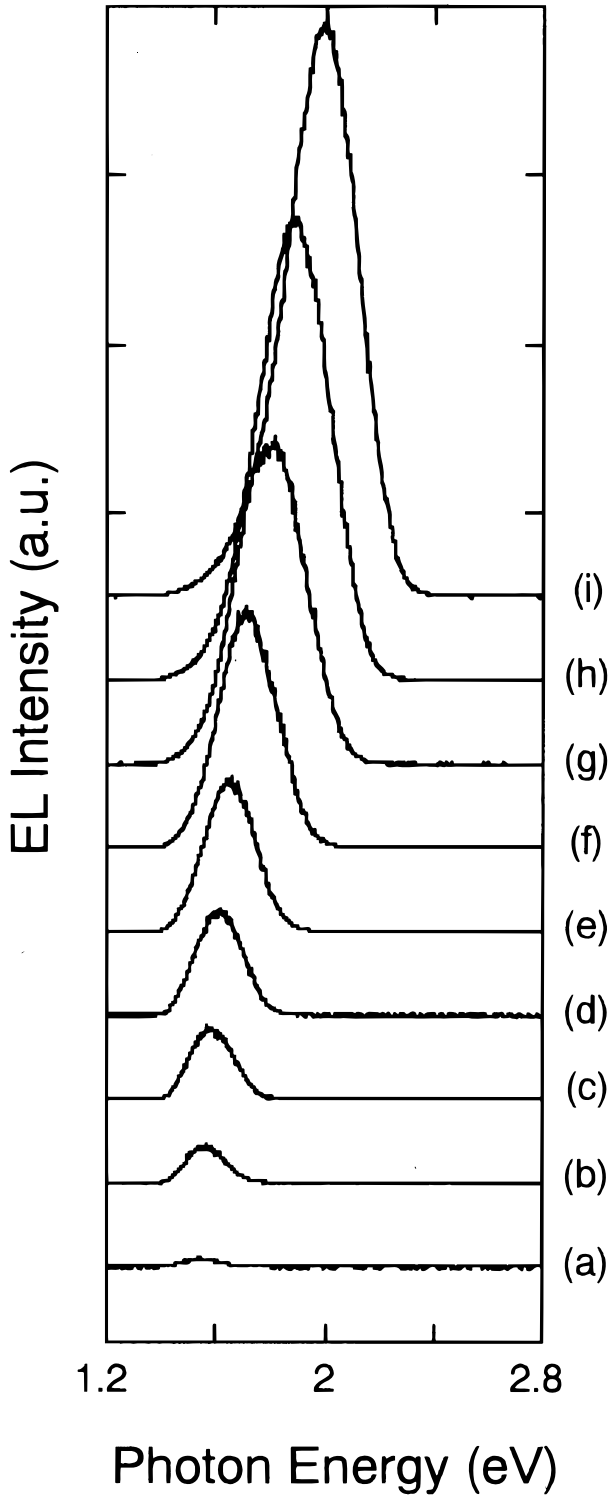


Figure 9. Time-resolved EL spectra obtained in 0.2 M Na_2SO_4 and 0.15 M $K_2S_2O_8$ solution when the potential was stepped for 1 s from 0 to −2.0 V. EL spectra were obtained every 0.1 s; (a) 0-0.1 s, (b) 0.1-0.2 s, (c) 0.2-0.3 s, (d) 0.3-0.4 s, (e) 0.4-0.5 s, (f) 0.5-0.6 s, (g) 0.6-0.7 s, (h) 0.7-0.8 s, and (i) 0.8-0.9 s. The n-PS samples were prepared by anodic oxidation in 10% HF-ethanol at 5 mA/cm^2 for 300 s.

Downloaded on 2012-09-26 to IP 133.87.26.18 address. Redistribution subject to ECS license or copyright; see www.esltbd.org

S0013-4651(99)04-064-1 CCC: $7.00 © The Electrochemical Society, Inc.

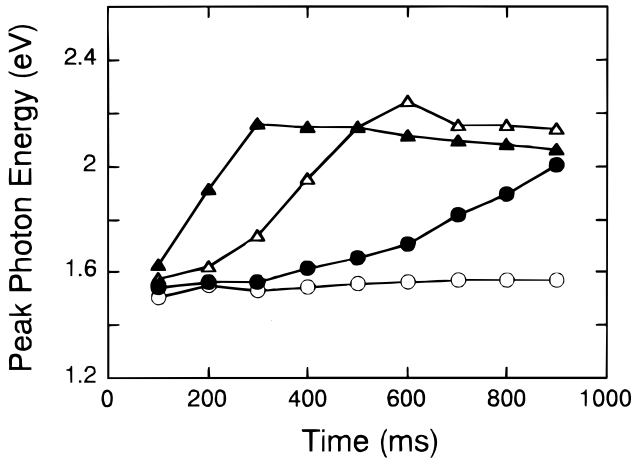


Figure 10. The dependence of peak energy obtained from the time-resolved EL spectra with time after stepping the potential. Potential was stepped from 0 to (○) −1.5, (●) −2.0, (△) −2.5, and (▲) −3.0. PS samples were prepared by anodic oxidation in 10% HF-ethanol at 5 mA/cm^2 for 300 s.

respectively, in all cases, suggests that the n-PS prepared under the present conditions consisted of nanometer-sized Si crystallites with bandgap energies from *ca*. 1.4 to *ca*. 2.6 eV (Fig. 8). Theoretical calculation shows that nanometer-sized Si crystallites with bandgap energies from 1.4 to 2.6 eV have diameters of *ca*. 4.5 to *ca*. 2.0 nm.[55]

The crystallites in PS are reported to be distributed vertically from a smaller size at the PS/electrolyte solution interface to a larger size at the PS/Si interface,[56] *i.e.*, the bandgap energy is distributed from larger at the top to smaller at the bottom of the PS layer. The larger sized Si crystallites at the bottom and the smaller sized Si crystallites at the top of the PS layer should emit EL of longer wavelength (lower energy) and shorter wavelength (higher energy), respectively. Thus, the time-dependent blue shift of the EL spectra can be explained by considering that the rate of the EL generation depends on the size of the Si crystallites in the PS layer, *i.e.*, the major reaction site at the initial stage of the potential pulse was near the n-PS/Si interface where the size of the Si crystallites is large, and the fact that the reaction sites moved gradually to the top of the n-PS layer with the time needed to build up a homogeneous electric field through the PS layer.

Conclusions

Visible EL from n-PS in an electrolyte solution containing $S_2O_8^{2-}$ was investigated by potential-sweep and potential-step methods. By potential-sweep measurements, we found a dependence of EL intensity, cathodic current, and EL spectra on the scan rate. By potential-step measurements, the EL intensity was found to increase with increasing cathodic polarization time although the cathodic current decreased. By time-resolved EL spectra measurements, we found that the EL spectrum was blue-shifted even at a constant negative potential applied to n-PS. We concluded from these results that the emission site changed from larger sized Si crystallites to smaller sized ones in the n-PS layer. We proposed for the first time a mechanism in which the EL process was dependent not only on the electrode potential but also on the time after the negative potential was applied.

Acknowledgment

This work was partially supported by Grants-in-Aid for Scientific Research on Priority Area of “Electrochemistry of Ordered Interface” from the Ministry of Education, Science, Sports, and Culture, Japan. We are grateful to Mr. Kitazawa of Shin-Etsu Semiconductor for the donation of Si wafers. H.N. acknowledges the Japan Society for the Promotion of Science for the JSPS Research Fellowships for Young Scientists.

Hokkaido University assisted in meeting the publication costs of this article.

References

1. L. T. Canham, *Appl. Phys. Lett.*, **57**,1046 (1990).
2. N. Koshida and H. Koyama, *Appl. Phys. Lett.*, **60**, 347 (1992).
3. A. Richter, W. Lang, P. Steiner, F. Kozlowski, and H. Sandmier, *Mater. Res. Soc.*, **256**, 209 (1992).
4. F. Namavar, H. P. Marusaka, and N. M. Kalahoran, *Appl. Phys. Lett.*, **60**, 2514 (1992).
5. T. Futagi, T. Matsumoto, M. Katsumoto, Y. Ohta, H. Mimura, and K. Kitamura, *Jpn. J. Appl. Phys.*, **31**, L616 (1992).
6. K. D. Hirschman, L. Tsybeskov, S. P. Duttagupta, and P. M. Fauchet, *Nature*, **384**, 338 (1996).
7. R. T. Collins, P. M. Fauchet, and M. A. Tischler, *Phys. Today*, **50**, 24 (1997).
8. V. Lehmann and U. Gösele, *Appl. Phys. Lett.*, **58**, 856 (1991).
9. T. Takagahara and K. Takeda, *Phys. Rev. B*, **46**, 15578 (1992).
10. Y. Kanemitsu, H. Uto, Y. Masumoto, T. Matsumoto, T. Futagi, and H. Mimura, *Phys. Rev. B*, **48**, 2827 (1993).
11. M. S. Brant, H. D. Fuchs, M. Stutzmann J. Weber, and M. Cardona, *Solid State Commun.*, **81**, 307 (1992).
12. H.-J. Lee, Y. H. Seo, D.-H. Oh, K. S. Nahm, Y. B. Hahn, I. C. Jeon, E.-K. Suh, Y. H. Lee, and H. J. Lee, *J. Appl. Phys.*, **75**, 8060 (1994).
13. S. M. Prokers, O. J. Glembocki, V. M. Bermundez, R. Kaplan, L. E. Friedersdorf, and P. C. Searson, *Phys. Rev. B*, **45**, 13788 (1992).
14. J. L. Gole, F. P. Dudel, L. Seals, M. Reiger, P. Kohl, and L. A. Bottomley, *J. Electrochem. Soc.*, **145**, 3284 (1998).
15. H. Koyama, M. Araki, Y. Yamamoto, and N. Koshida, *Jpn. J. Appl. Phys.*, **30,** 3606 (1991).
16. A. Bsiesy, J. C. Vial, F. Gaspard, R. Herino, M. Ligeon, F. Muller, R. Romestain, A. Wasiela, A. Halimaoui, and G. Bomchil, *Surf. Sci.*, **254**, 195 (1991).
17. M. A. Tischler, R. T. Collins, J. H. Stathis, and J. C. Tsang, *Appl. Phys. Lett.*, **60**, 639 (1992).
18. T. Matsumoto, M. Daimon, and T. Futagi, *Jpn. J. Appl. Phys.*, **31**, L619 (1992).
19. D. L. Fisher, J. Harper, and M. J. Sailor, *J. Am. Chem. Soc.*, **117**, 7846 (1995).
20. J. E. Song and M. J. Sailor, *J. Am. Chem. Soc.*, **119**, 7381 (1997).
21. M. A. Hory, A. Bsiesy, R. Herino, M. Ligeon, F. Muller, and J. C. Vial, *Thin Solid Films*, **276**, 130 (1996).
22. H. Noguchi, T. Kondo, and K. Uosaki, *J. Phys. Chem.*, **101**, 4678 (1997).
23. H. H. Streckert, B. R. Karas, D. J. Morano, and A. B. Ellis, *J. Phys. Chem.*, **84**, 3232 (1980).
24. K. Uosaki and H. Kita, *Bull. Chem. Soc. Jpn.*, **57**, 3247 (1984).
25. K. Uosaki and H. Kita, *J. Phys. Chem.*, **88**, 4197 (1984).
26. K. Uosaki and H. Kita, *J. Lumin.*, **31/32**, 972 (1984).
27. K. Uosaki and H. Kita, *J. Am. Chem. Soc.*, **108**, 4294 (1986).
28. K. Uosaki, *Trends Anal. Chem.*, **9**, 98 (1990).
29. A. Halimaoui, C. Oules, G. Bomchil, A. Bsiesy, F. Gaspard, R. Herino, M. Ligeon, and F. Muller, *Appl. Phys. Lett.*, **59**, 304 (1991).
30. S. Billat, *J. Electrochem. Soc.*, **143**, 1055 (1996).
31. E. S. Kooij, A. R. Rama, and J. J. Kelly, *Surf. Sci.*, **370**, 125 (1997).
32. J. D. Moreno, R. G-Lemus, J. M. M-Duart, M. L. Marcos, and J. G-Velasco, *J. Electroanal. Chem.*, **437**, 135 (1997).
33. T. Kondo, Y. Y. Kim, and K. Uosaki, *Denki Kagaku*, **62**, 540 (1994).
34. K. Uosaki, T. Kondo, H. Noguchi, K. Murakoshi, and Y. Y. Kim, *J. Phys. Chem.*, **100**, 4564 (1996).
35. E. S. Kooij, K. Butter, and J. J. Kelly, *J. Electrochem. Soc.*, **145**, 1232 (1998).
36. K. Murakoshi and K. Uosaki, *Appl. Phys. Lett.*, **62**, 1676 (1993).
37. L. T. Canham, W. Y. Leong, M. I. J. Beale, T. I. Cox, and L. Taylor, *Appl. Phys. Lett.*, **61**, 2563 (1992).
38. P. M. M. C. Bressers, J. W. J. Knapen, E. A. Meulenkamp, and J. J. Kelly, *Appl. Phys. Lett.*, **61**, 108 (1992).
39. E. A. Meulenkamp, P. M. M. C. Bressers, and J. J. Kelly, *Appl. Surf. Sci.*, **64**, 283 (1993).
40. A. Bsiesy, F. Muller, M. Ligeon, F. Gaspard, R. Herino, R. Romestain, and J. C. Vial, *Phys. Rev. Lett.*, **71**, 637 (1993).
41. A. Bsiesy, J. C. Vial, F. Gaspard, R. Herino, M. Ligeon, I. Mihalcescu, F. Muller, and R. Romestain, *J. Electrochem. Soc.*, **141**, 3071 (1994).
42. E. A. Meulenkamp, L. M. Peter, D. J. Riley, and R. I. Wielgosz, *J. Electroanal. Chem.*, **392**, 97 (1995).
43. L. M. Peter, D. J. Riley, R. I. Wielgosz, P. A. Snow, R. V. Penty, I. H. White, and E. A. Meulenkamp, *Thin Solid Films*, **276**, 123 (1996).
44. K. Ogasawara, T. Momma, and T. Osaka, *J. Electrochem. Soc.*, **142**, 1874 (1995).
45. K. Ogasawara, T. Momma, and T. Osaka, *Chem. Lett.*, 1243 (1995).
46. K. Uosaki, H. Noguchi, K. Murakoshi, and T. Kondo, *Chem. Lett.*, 667 (1995).
47. E. S. Kooij, S. M. Noordhoek, and J. J. Kelly, *J. Phys. Chem.*, **100**, 10754 (1996).
48. J.-E. Lim, W.-S. Chae, Y. Lee, and K.-J. Kim, *J. Electrochem. Soc.*, **144**, 647 (1997).
49. R. Memming, *J. Electrochem. Soc.*, **116**, 785 (1969).
50. A. Halimaoui, *Appl. Phys. Lett.*, **63**, 1264 (1993).
51. R. Herino, G. Bomchil, K. Barla, C. Bertrand, and J. L. Ginoux, *J. Electrochem. Soc.*, **134**, 1994 (1987).
52. A. J. Bard and L. R. Faulkner, *Electrochemical Methods*, John Wiley & Sons, New York (1980).
53. B. Gelloz, A. Bsiesy, F. Gaspard, and F. Muller, *Thin Solid Films*, **276**, 175 (1996).
54. L. M. Peter, D. J. Riley, and R. I. Wielgosz, *Appl. Phys. Lett.*, **66**, 2355 (1995).
55. J. P. Proot, C. Delerue, and G. Allan, *Appl. Phys. Lett.*, **61**, 1948 (1992).
56. K. Takemoto, Y. Nakamura, and O. Nittono, *Jpn. J. Appl. Phys.*, **33**, 6432 (1994).

Downloaded on 2012-09-26 to IP 133.87.26.18 address. Redistribution subject to ECS license or copyright; see www.esltbd.org